Supporting Information

Theoretical exploration on activity of copper single-atom catalyst for electrocatalytic reduction of CO_2

Junyong Min[a,b], Lei Liu[c], Fengjuan Chen[a,*], Xuekun Jin[d], Tianjiao Yuan[b], Xiaoqian Yao[b,*]

[a] Key Laboratory of Solid State Physics and Devices Autonomous Region, School of Physics Science and Technology, Xinjiang University, Urumqi 830046, Xinjiang, P. R. China

[b] Beijing Key Laboratory of Ionic Liquids Clean Process, CAS Key Laboratory of Green Process and Engineering, State Key Laboratory of Multiphase Complex Systems, Institute of Process Engineering, Chinese Academy of Sciences, Beijing 100190, P.R. China

[c] Center for Computational Chemistry, College of Chemistry and Chemical Engineering, Wuhan Textile University, Wuhan, 430200, China

[d] School of Environment, Tsinghua University, Beijing 100084, P. R. China

Contents

and the formation energy (E_f) are in eV, and the solvation potential (U_{diss}) is in V.

15. Table S2: Calculated standard potentials for reactions given by Eq. (1) to (4), standard conditions, 298 K, pH = 0.
16. Table S3: The adsorption energy corresponding to the position number of the hydrogen proton adsorbed on CuN_3V.
17. Table S4: The adsorption energy corresponding to the position number of the hydrogen proton adsorbed on CuN_2V_2.
18. Table S5: The CO_2RR and HER transition state energy barriers for hydrogen proton adsorption at different sites on CuN_3V.
19. Table S6: The adsorption energy corresponding to the position of multiple hydrogen protons adsorbed on CuN_3V.
20. Table S7: Average bond lengths (d_{Cu-N} and $d_{Cu-C)}$ of Cu-N and Cu-C (*COOH), Bader charge transfer of Cu atoms (Q_{Cu}), and d-band center of Cu atoms (ε_d) of the catalysts for CuN_4, CuN_3V, and CuN_2V_2 without adsorbed intermediates and after adsorption of COOH. The bond lengths are in Å, the Bader charges are in e^-, and the d-band centers are in eV.

Calculation method

The adsorption energy is calculated by:

$$\Delta E_{ads} = E_{total} - (E_{adsorbate} + E_{slab})$$

where E_{total}, E_{slab} and $E_{adsorbate}$ represent the energy containing the catalyst adsorbate, catalyst and adsorbate, respectively.

The formula for calculating the free energy of adsorption of reactants or intermediates:

$$\Delta G_{ads} = \Delta E_{ads} + \Delta ZPE - T\Delta S$$

where ΔE_{ads} is calculated from the adsorption energy equation, ΔZPE and ΔS are the zero-point energy and entropy changes at 298.15 K, which are calculated from the vibrational frequency, and the entropy of the gas-phase molecules from the NIST database.

Equation for the change in Gibbs free energy (ΔG) of CO_2RR:

$$\Delta G = \Delta E + \Delta ZPE - T\Delta S + \Delta G_{pH} + \Delta G_{U}$$

where ΔE is the reaction energy difference of the reaction step in CO_2RR, which can be obtained directly from the DFT calculation, and ΔZPE and ΔS are the same values as in the adsorption free energy equation; ΔG_{pH} is the free energy correction for pH, which is zero in this work; and $\Delta G_U = -eU$, where U is the electrode potential of the electrochemical step.

The binding energy (E_b) is calculated as:

$$E_b = E_{M-N/C} - E_{N-C} - E_M$$

where $E_{M-N/C}$, E_{N-C} and E_M are the structure after anchoring the metal atom, the structure without anchoring the metal atom and the energy of the metal single atom, respectively.

The cohesive energy (E_c) is calculated as:

$$E_c = E_{bulk} - E_M$$

where E_{bulk} is the energy of a single metal atom in the bulk phase.

The energy of formation (E_f) is calculated as:

$$E_f = E_{M-N/C} + n_C\mu_C - (E_{V-gra} + n_N\mu_N + E_{bulk})$$

where n_C and n_N are the number of C atoms replaced by N atoms and the number of nitrogen atoms in the catalyst, respectively, μ_C and μ_N are the chemical potentials of C and N, respectively, corresponding to the energy of a single C atom in bulk-phase graphene and the energy of a single N atom in nitrogen, and E_{V-gra} is the energy of the graphene structure without the intercalated N and metal atoms.

The dissolution potential (U_{diss}) is calculated as:

$$U_{diss} = U^{\circ}_{diss} - \frac{E_f}{ne^-}$$

where U°_{diss} is the standard dissolution potential of the metal and n is the number of electrons involved in the dissolution (n=2).

The d-band center of the catalyst is calculated as:

$$\varepsilon_d = \frac{\int_{-\infty}^{\infty} n_d(\varepsilon)\varepsilon \, d\varepsilon}{\int_{-\infty}^{\infty} n_d(\varepsilon) \, d\varepsilon}$$

where $n_d(\varepsilon)$ represents the total d state of the copper atoms in Cu-N/C.

we consider the following surface electrochemical process on model Cu-N/C:

$$Cu^{2+} + 2e^- + N/C \rightarrow Cu\text{-}N/C \qquad (1)$$

$$\mathrm{Cu\text{-}N/C + H^+ + e^- \rightarrow H\text{-}Cu\text{-}N/C} \quad (2)$$

$$\mathrm{OH\text{-}Cu\text{-}N/C + H^+ + e^- \rightarrow Cu\text{-}N/C + H_2O} \quad (3)$$

$$\mathrm{O\text{-}Cu\text{-}N/C + 2H^+ + 2e^- \rightarrow Cu\text{-}N/C + H_2O} \quad (4)$$

The electromotive force of a hypothetical galvanic cell is obtained by dividing calculated ΔG (in eV) by the number of electrons exchanged in the reaction. Taking that the anode is SHE (E° = 0 V), the obtained values are numerically equal to the standard electrode potentials for reactions (2)-(4). For the construction of the surface Pourbaix plots, the activity (a) of Cu^{2+} ions was taken to be 1×10^{-8} mol·dm^{-3}. This is a typical value for construction of Pourbaix plots and the change of Cu^{2+} concentration by one order of magnitude only shifts the potential of Eq. (1) vertically along the potential axis of a given Pourbaix plot by 0.059 V (at room temperature).

We constructed surface Pourbaix plots for the studied model Cu-N/C at standard conditions and at 298 K. Considered surface processes include:

(i) metal dissolution, Eq. (1), with Nernst equation:

$$\mathrm{E(Cu^{2+}/Cu\text{-}N/C) = E^\circ(Cu^{2+}/Cu\text{-}N/C) - (0.059/2) \times \log a(Cu^{2+})} \quad (5)$$

(ii) hydrogen deposition, Eq. (2), with Nernst equation:

$$\mathrm{E(H\text{-}Cu\text{-}N/C/Cu\text{-}N/C) = E^\circ(H\text{-}Cu\text{-}N/C/Cu\text{-}N/C) - 0.059 \times pH} \quad (6)$$

(iii) Cu-N/C oxidation via deposition of OH_{ads}, Eq. (3), with Nernst equation:

$$\mathrm{E(OH\text{-}Cu\text{-}N/C/Cu\text{-}N/C) = E^\circ(OH\text{-}Cu\text{-}N/C/Cu\text{-}N/C) - 0.059 \times pH} \quad (7)$$

(iv) Cu-N/C oxidation via deposition of O_{ads}, Eq. (4), with Nernst equation:

$$\mathrm{E(O\text{-}Cu\text{-}N/C/Cu\text{-}N/C) = E^\circ(O\text{-}Cu\text{-}N/C/Cu\text{-}N/C) - 0.059 \times pH} \quad (8)$$

The calculated standard potentials (E°(O/R)) are summarized in Table S2. Metal dissolution, Eq. (1) is not pH-dependent, but H_{ads}, OH_{ads}, and O_{ads} formation are, with the slope of the equilibrium potential versus pH line of 0.059 mV per pH unit in all the cases. When the equilibrium potentials were calculated using Eqs. (5)-(8) for pH ranging from 0 to 14, the stable phases were identified following the rule that the most stable oxidized phase had the lowest equilibrium potential, while the most stable reduced phase was the one with the highest equilibrium potential.

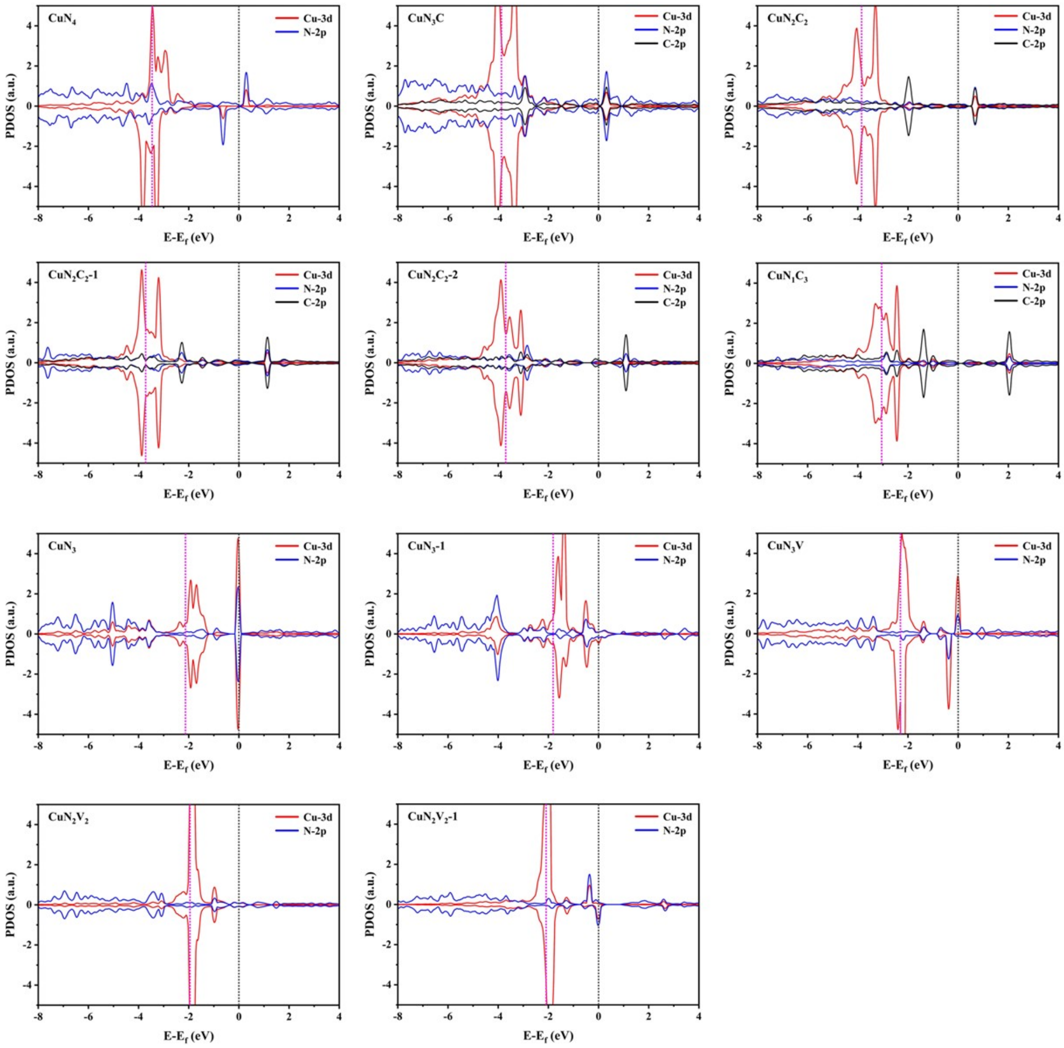

Fig. S1 Electron density of states diagram for 11 kinds of catalysts; pink dashed line: d-band center of Cu atom, gray dashed line: Fermi energy level.

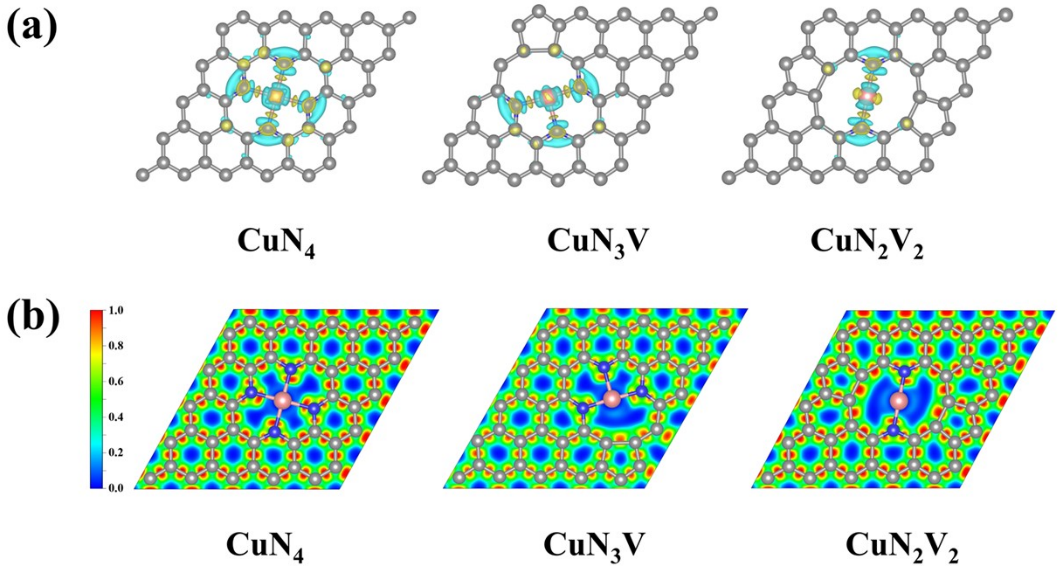

Fig. S2 CuN_4 CuN_3V and CuN_2V_2 for (a) charge density difference, (b) electron localization function. The iso-surface value was set to be 0.005 $e \cdot Å^{-3}$ and the positive and negative charges are shown in yellow and cyan, respectively.

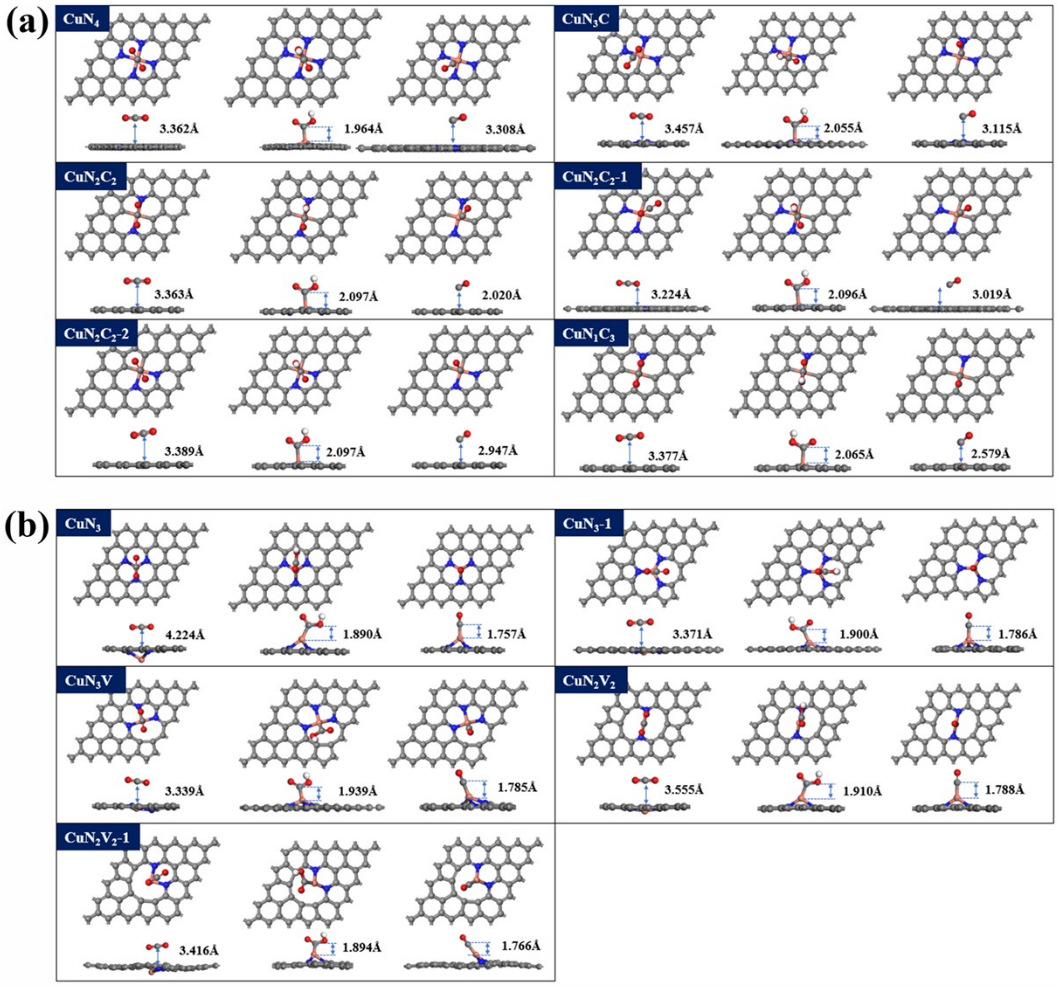

Fig. S3 Optimized geometries of CO_2RR adsorbates on (a) saturated coordination catalysts and (b) unsaturated coordination catalysts.

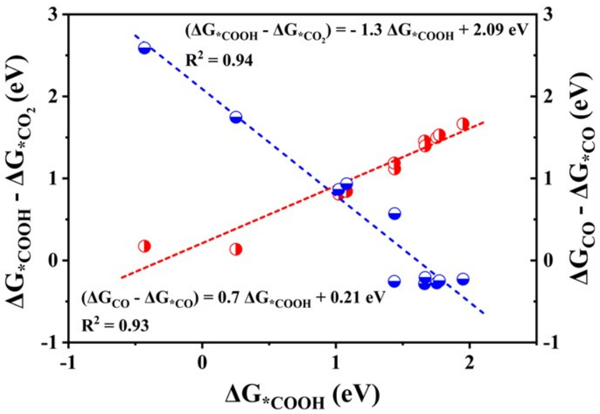

Fig. S4 Linear scaling relationships for ΔG_{*COOH} and (ΔG_{CO} - ΔG_{*CO}), (ΔG_{*COOH} - ΔG_{*CO2}).

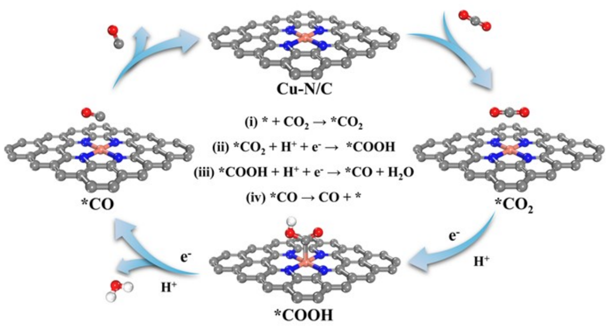

Fig. S5 Schematic diagram of the reaction process for the reduction of CO_2 to CO on CuN_4.

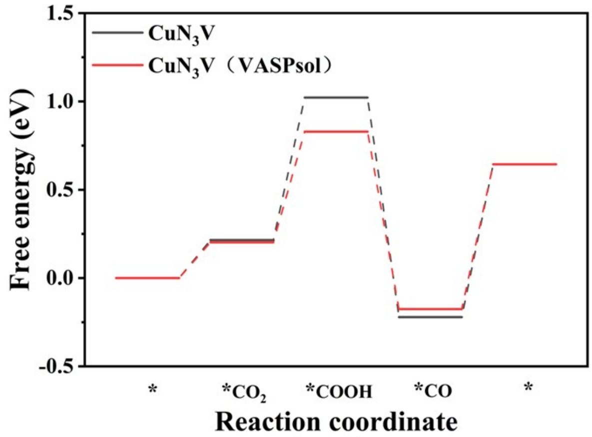

Fig. S6 Gibbs free energy (ΔG) diagram of CO_2RR on CuN_3V with the addition of the implicit solvent model.

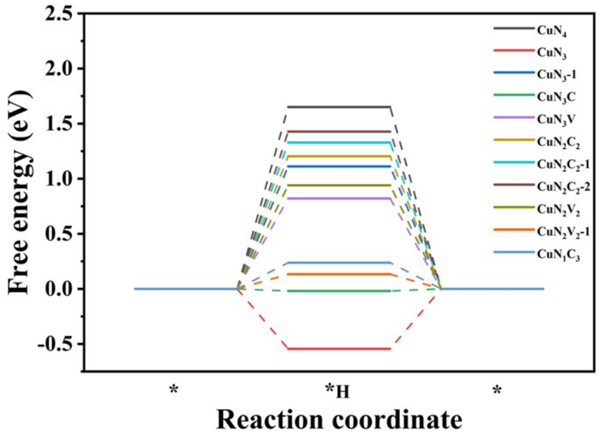

Fig. S7 HER free energy diagram for single-atom Cu (Cu-N/C) catalysts.

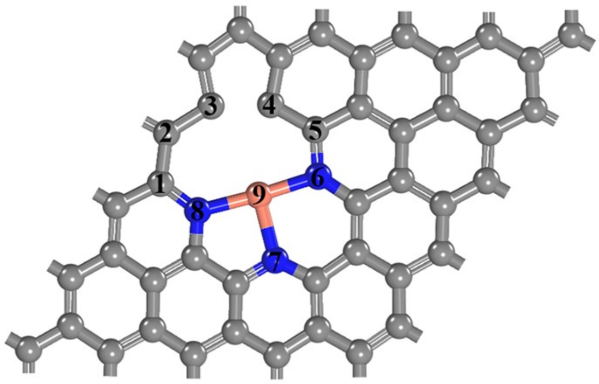

Fig. S8 Position number of hydrogen protons adsorbed on CuN_3V.

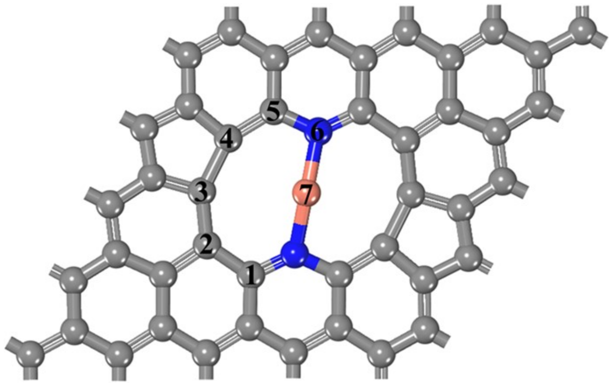

Fig. S9 Position number of hydrogen protons adsorbed on CuN_2V_2.

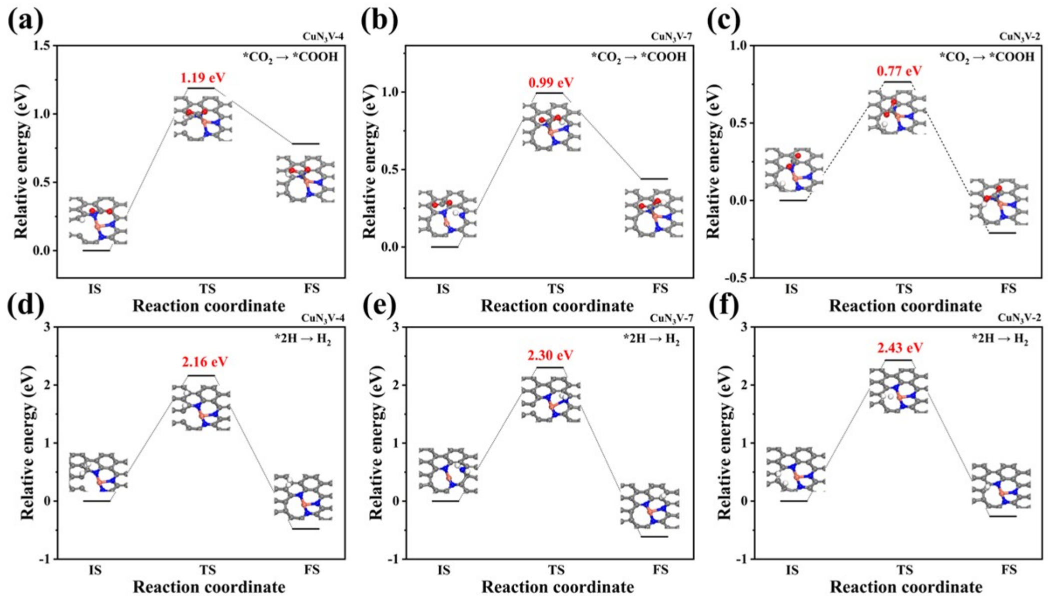

Fig. S10 CO_2RR (a, b and c) and HER (d, e and f) transition states of hydrogen protons adsorbed at sites 4, 7 and 2 on CuN_3V.

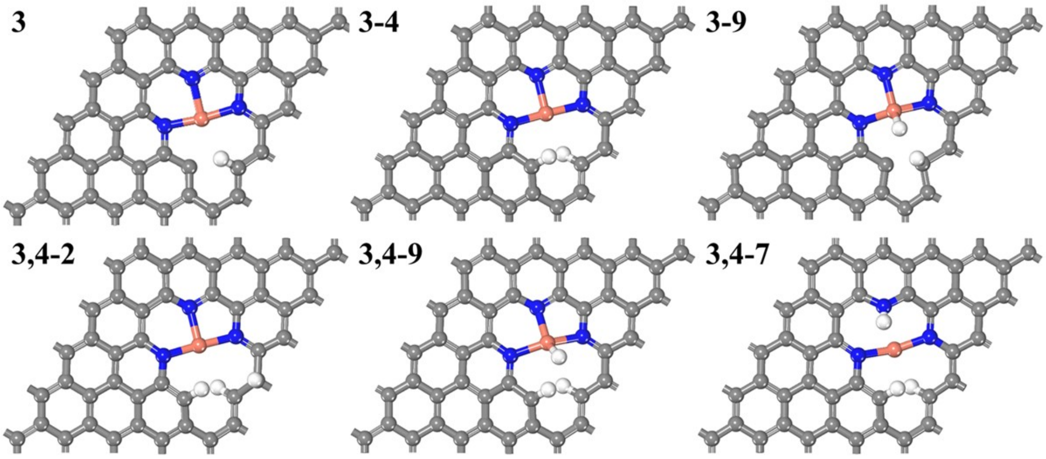

Fig. S11 The adsorption configurations of multiple hydrogen protons on CuN_3V with their corresponding numbers.

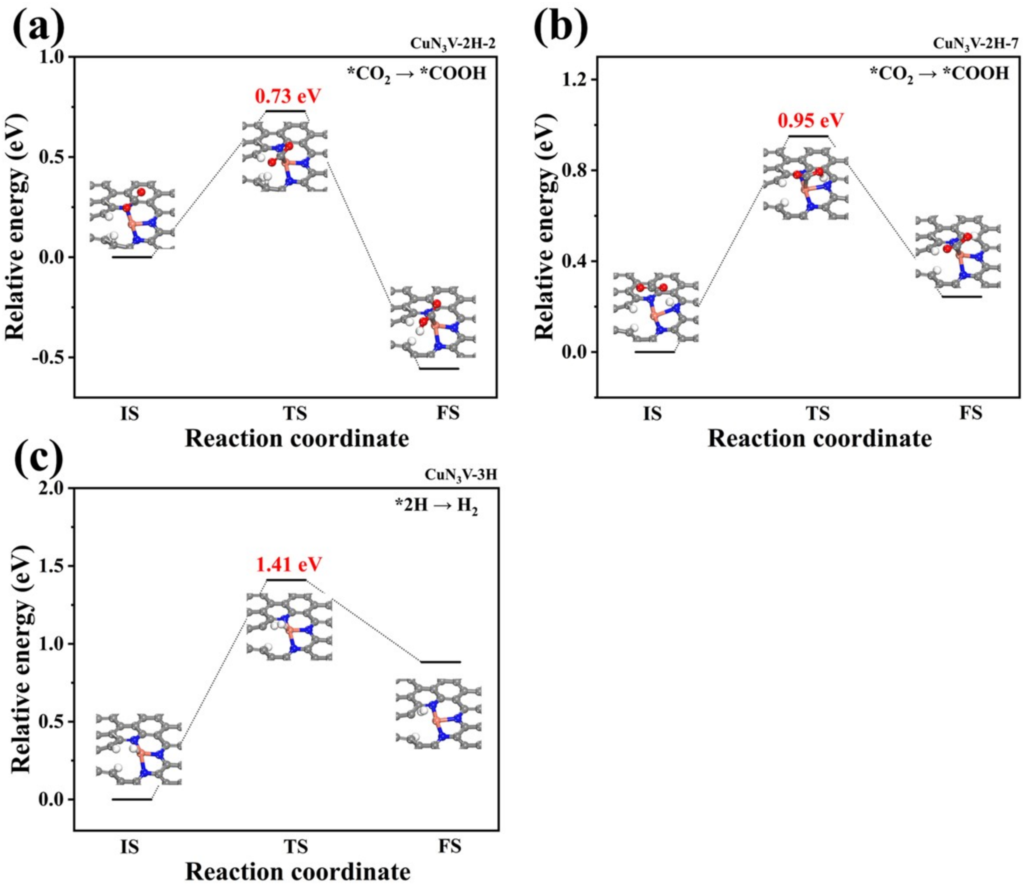

Fig. S12 Transition state energy barriers of (a) and (b) *CO_2 to *COOH, (c) HER on CuN_3V saturated by hydrogen protons.

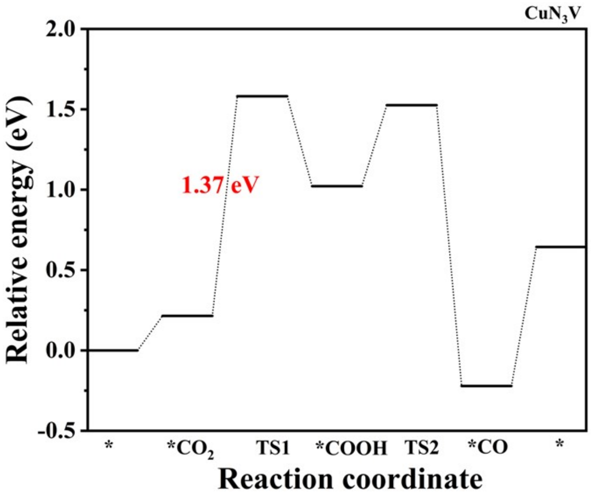

Fig. S13 Transition state energy barrier for all of CO_2RR on CuN_3V

Table S1 Average bond length ($d_{Cu\text{-}N}$), Bader charge transfer (Q_{Cu} and Q_N), binding energy (E_b), the d-band center of Cu atoms (ε_d), binding energy, (E_b) formation energy (E_f), and solvation potential (U_{diss}) for Cu-N catalysts. The bond length is in Å, the Bader charge is in e^-, the d-band center, the binding energy (E_b), and the formation energy (E_f) are in eV, and the solvation potential (U_{diss}) is in V.

System	$\mathbf{d_{Cu\text{-}N}}$	$\mathbf{Q_{Cu}}$	$\mathbf{Q_N}$	$\boldsymbol{\varepsilon_d}$	$\mathbf{E_b}$	$\mathbf{E_f}$	$\mathbf{U_{diss}}$
CuN_4	1.93	-0.92	1.21	-3.46	-5.42	-7.80	4.24
CuN_3C	1.91	-0.85	1.19	-3.87	-7.75	-6.77	3.72
CuN_2C_2	1.91	-0.81	1.15	-3.85	-8.46	-5.73	3.21
CuN_2C_2-1	1.91	-0.77	1.22	-3.72	-8.69	-5.80	3.24
CuN_2C_2-2	1.93	-0.74	1.22	-3.77	-9.59	-6.28	3.48
CuN_1C_3	1.94	-0.71	1.20	-3.05	-8.97	-5.03	2.86
CuN_3	1.72	-0.63	1.27	-2.13	-4.26	-5.10	2.89
CuN_3-1	1.81	-0.73	1.10	-1.81	-7.34	-9.24	4.96
CuN_3V	1.88	-0.74	1.28	-2.30	-5.88	-7.77	4.23
CuN_2V_2	1.75	-0.58	1.22	-1.95	-6.71	-7.32	4.00
CuN_2V_2-1	1.93	-0.79	1.25	-2.09	-5.32	-3.20	1.94

Table S2 Calculated standard potentials for reactions given by Eq. (1) to (4), standard conditions, 298 K, pH = 0.

System	E°(Cu^{2+}/Cu-N/C)/V	E°(Cu-N/C /H-Cu-N/C)/V	E°(O-Cu-N/C/ Cu-N/C)/V	E°(OH-Cu-N/C/ Cu-N/C)/V
CuN_4	1.06	-1.65	1.96	1.76
CuN_3	0.49	0.54	0.49	-0.66
CuN_3C	2.23	0.02	0.62	1.73
CuN_3V	1.30	-0.82	1.42	0.91
CuN_3-1	2.02	-1.11	1.59	1.41
CuN_2C_2	2.58	-1.20	2.01	1.73
CuN_2C_2-1	2.70	-1.33	2.11	1.80
CuN_2C_2-2	3.15	-1.43	2.03	1.66
CuN_2V_2	1.71	-0.94	1.39	0.79
CuN_2V_2-1	1.01	-0.13	0.91	-0.13
CuN_1C_3	2.83	-0.24	0.74	2.25

Table S3 The adsorption energy corresponding to the position number of the hydrogen proton adsorbed on CuN_3V.

***H**	1(C)	2(C)	3(C)	4(C)	5(C)	6(N)	7(N)	8(N)	9(Cu)
ΔE_{ads}(eV)	0.97	0.63	-0.56	-0.40	0.89	0.66	0.22	0.80	0.62

Table S4 The adsorption energy corresponding to the position number of the hydrogen proton adsorbed on CuN_2V_2.

***H**	1	2	3	4	5	6	7
ΔE_{ads}(eV)	0.84	0.57	-0.10	-0.18	0.92	0.50	0.77

Table S5 The CO_2RR and HER transition state energy barriers for hydrogen proton adsorption at different sites on CuN_3V.

***H-site**	4	7	2
CO_2RR (eV)	1.19	0.99	0.77
HER (eV)	2.16	2.30	2.43

Table S6 The adsorption energy corresponding to the position of multiple hydrogen protons adsorbed on CuN_3V.

***H**	3	3-4	3-9	3,4-2	3,4-9	3,4-7
ΔE_{ads}(eV)	-0.56	-1.89	0.90	1.36	0.90	0.58

Table S7 Average bond lengths (d_{Cu-N} and d_{Cu-C}) of Cu-N and Cu-C (*COOH), Bader charge transfer of Cu atoms (Q_{Cu}), and d-band center of Cu atoms (ε_d) of the catalysts for CuN_4, CuN_3V, and CuN_2V_2 without adsorbed intermediates and after adsorption of COOH. The bond lengths are in Å, the Bader charges are in e^-, and the d-band centers are in eV.

System	Q_{Cu}	d_{Cu-N}	ε_d	d_{Cu-C}
CuN_4	-0.92	1.93	-3.46	\
CuN_4-COOH	-0.87	2.01	-2.71	1.96
CuN_3V	-0.74	1.88	-2.30	\
CuN_3V-COOH	-0.82	1.95	-2.44	1.94
CuN_2V_2	-0.58	1.75	-1.95	\
CuN_2V_2-COOH	-0.73	1.97	-2.22	1.91